PERGAMON International Journal of Engineering Science 37 (1999) 1723–1736

International Journal of Engineering Science

www.elsevier.com/locate/ijengsci

Unsteady flow and heat transfer on a semi-infinite flat plate with an aligned magnetic field

H.S. Takhar [a,*], A.J. Chamkha [b], G. Nath [c]

[a] *School of Engineering, University of Manchester, Manchester, M13 9PL, UK*
[b] *Department of Mechanical Engineering, Kuwait University, Safat 13060, Kuwait*
[c] *Department of Mathematics, Indian Institute of Science, Bangalore 560012, India*

Received 13 March 1998; accepted 15 July 1998

(Communicated by E.S. ŞUHUBİ)

Abstract

The unsteady laminar boundary layer flow of an electrically conducting fluid past a semi-infinite flat plate with an aligned magnetic field has been studied when at time $t > 0$ the plate is impulsively moved with a constant velocity which is in the same or opposite direction to that of free stream velocity. The effect of the induced magnetic field has been included in the analysis. The non-linear partial differential equations have been solved numerically using an implicit finite-difference method. The effect of the impulsive motion of the surface is found to be more pronounced on the skin friction but its effect on the x-component of the induced magnetic field and heat transfer is small. Velocity defect occurs near the surface when the plate is impulsively moved in the same direction as that of the free stream velocity. The surface shear stress, x-component of the induced magnetic field on the surface and the surface heat transfer decrease with an increasing magnetic field, but they increase with the reciprocal of the magnetic Prandtl number. However, the effect of the reciprocal of the magnetic Prandtl number is more pronounced on the x-component of the induced magnetic field.

1. Introduction

The study of the boundary layer behaviour on continuous surfaces is important because the analysis of such flows finds applications in different areas such as the aerodynamic extrusion of a plastic sheet, the cooling of a metallic plate in a cooling bath, the boundary layer along material

* Corresponding author. Tel.: 0044-161-275-4361; fax: 0044-161-275-4356.
E-mail address: hstakhar@man.ac.uk (H.S. Takhar)

0020-7225/99/$ – see front matter
PII: S0020-7225(98)00144-X

handling conveyers, and the boundary layer along a liquid film in condensation processes. Sakiadis [1] has studied the boundary layer on a continuous semi-infinite sheet moving steadily through an otherwise quiescent fluid environment. The boundary layer solution of Sakiadis [1] resulted in a skin friction of about 30% higher than that of Blasius [2] for the flow past a stationary semi-infinite flat plate. The steady laminar incompressible flow of a viscous electrically conducting fluid with constant properties past a semi-infinite flat plate with aligned magnetic field without heat transfer has been studied by Greenspan and Carrier [3], Glauert [4], Gribben [5] and Na [6]. The corresponding heat transfer problem has been considered by Tan and Wang [7] and Afzal [8]. The above studies deal with the steady flows only. It is known that almost all the flow problems encountered in practice are unsteady. The steady flow over a continuous moving surface with a magnetic field has been studied by Vajravelu [9] and Takhar et al. [10]. The unsteady boundary layer flow over a stationary semi-infinite flat plate in the presence of a magnetic field has been studied by Das [11], Ingham [12] and Goyal and Bansal [13] when the free stream velocity is changed impulsively.

The present analysis deals with the unsteady flow and heat transfer over a semi-infinite flat plate with an aligned magnetic field when at time $t > 0$ the plate is impulsively moved with a constant velocity. At time $t = 0$ the flat plate was stationary and there was a steady flow over it due to the free stream velocity u_∞. The effect of the induced magnetic field has been included in the analysis. The governing partial differential equations have been solved numerically using an implicit finite-difference scheme [14]. Particular cases of the present results have been compared with those available in the literature [4,6,7,11].

2. Analysis

Let us consider that at $t = 0$, there is a steady laminar incompressible viscous electrically conducting fluid of constant properties flowing past a fixed semi-infinite unmagnetized and non-conducting plate having a constant free stream velocity u_∞. At $t > 0$, the plate is impulsively moved with constant velocity u_w which causes unsteadiness in the flow field (see inset of Fig. 1). The fluid has density ρ, kinematic viscosity ν, thermal diffusivity α ($= k/\rho\, c_p$), magnetic permeability μ_0 and magnetic diffusivity α_1 ($= (\mu_0\, \sigma)^{-1}$). All these quantities are supposed to be constant. A constant magnetic field H_0 is applied parallel to the plate outside the boundary layer. Let (u, v) and (H_1, H_2) be the velocity and the induced magnetic field components along and perpendicular to the plate. We assume that the normal component of the induced magnetic field H_2 vanishes at the wall and the parallel component H_1 approaches the given value H_0 at the edge of the boundary layer. It is also assumed that the viscous Reynolds number $\mathrm{Re} = u_\infty\, x/\nu$, and magnetic Reynolds number $\mathrm{Rm} = u_\infty\, x/\alpha_1$ are sufficiently large for momentum and magnetic boundary layers to have developed. Since the plate is semi-infinite in extent, the physical conditions depend only on the y and t variables. We further assume that no applied or polarisation voltages exist in the boundary layer, i.e. the electric field $\mathbf{E} = 0$. This then corresponds to the case when no energy is added or extracted from the fluid by electrical means. The magnetic effects are confined to retarding the flow and dissipating the energy of motion into heat. The viscous and Ohmic dissipation terms and the Hall effects have been neglected. The wall temperature T_w and the free stream temperature T_∞ are taken as being constant. Under the afore-mentioned assumptions the boundary layer

equations for the velocity, magnetic and temperature fields in the absence of electric field can be expressed as [11,15]:

$$u_x + v_y = 0, \tag{1}$$

$$(H_1)_x + (H_2)_y = 0, \tag{2}$$

$$u_t + uu_x + vu_y = vu_{yy} + (\mu_0/\rho)[H_1(H_1)_x + H_2(H_1)_y], \tag{3}$$

$$(H_1)_t + u(H_1)_x + v(H_1)_y - H_1u_x - H_2u_y = \alpha_1(H_1)_{yy}, \tag{4}$$

$$T_t + uT_x + uT_y = \alpha T_{yy}. \tag{5}$$

The boundary conditions for $t > 0$ are given by

$$\begin{aligned} &u = u_w, \quad v = H_2 = (H_1)_y = 0, \quad T = T_w \qquad \text{at } y = 0, \\ &u \to u_\infty, \quad H_1 \to H_0, \quad T \to T_\infty \qquad \text{as } y \to \infty. \end{aligned} \tag{6}$$

The initial conditions are given by the steady-state ($t = 0$) equations under boundary conditions (6) except that $u = 0$ at $y = 0$, instead of $u = u_w$ at $y = 0$.

Here x and y are, respectively, the distances along and perpendicular to the plate; u and v are the velocity components along x and y directions, respectively; t is the time; H_0 the applied magnetic field parallel to the x-axis in the free stream; H_1 and H_2 are the components of the induced magnetic field in the x and y directions, respectively; T is the temperature; ρ, ν and σ are, respectively, the density, kinematic viscosity and electrical conductivity; μ_0 is the magnetic permeability; Pr is the Prandtl number; α and α_1 are thermal and magnetic diffusivity, respectively; the subscripts t, x and y denote derivatives with respect to t, x and y, respectively; and the subscripts e and w denote conditions at the edge of the boundary layer and on the surface, respectively.

In order to reduce the number of independent variables from three to two and to make the governing equations dimensionless, we apply the following transformations:

$$\begin{aligned} &\eta = (u_\infty/\nu)^{1/2}x^{-1/2}y, \quad t^* = u_\infty t/x, \\ &u = u_\infty f'(\eta, t^*), \quad H_1 = H_0 g'(\eta, t^*), \quad \beta = \mu_0 H_0^2/\rho u_\infty^2, \\ &\psi = (u_\infty \nu)^{1/2} y^{1/2} f(\eta, t^*), \quad G(\eta, t^*) = (T - T_w)/(T_\infty - T_w), \\ &\phi = H_0(\nu x/u_\infty)^{1/2} g(\eta, t^*), \quad \lambda = \alpha_1/\nu, \quad \mathrm{Pr} = \nu/\alpha, \\ &u = \partial\psi/\partial y, \quad v = -\partial\psi/\partial x, \quad H_1 = \partial\phi/\partial y, \quad H_2 = -\partial\phi/\partial x, \\ &\varepsilon = u_w/u_\infty < 1 \end{aligned} \tag{7}$$

to Eqs. (1)–(5) and we find that Eqs. (1) and (2) are identically satisfied and Eqs. (3)–(5) reduce to

$$\begin{aligned} &2f''' + ff'' - \beta gg'' - 2\partial f'/\partial t^* + 2t^*[f'(\partial f'/\partial t^*) - (\partial f/\partial t^*)f''], \\ &\quad -2\beta t^*[g'(\partial g'/\partial t^*) - g''(\partial g/\partial t^*)] = 0, \end{aligned} \tag{8}$$

$$2\lambda g''' + (fg'' - f''g) - 2(\partial g'/\partial t^*) + 2t^*[f'(\partial g'/\partial t^*) - (\partial f/\partial t^*)g''], \\ -2t^*[g'(\partial f'/\partial t^*) - f''(\partial g/\partial t^*) = 0, \tag{9}$$

$$2\mathrm{Pr}^{-1}G'' + fG' - 2(\partial G/\partial t^*) + 2t^*[f'(\partial G/\partial t^*) - (\partial f/\partial t^*)G'] = 0. \tag{10}$$

The boundary conditions are given by

$$f(0,t^*) = 0, \quad f'(0,t^*) = \varepsilon, \quad g(0,t^*) = g''(0,t^*) = G(0,t^*) = 0, \\ f'(\infty,t^*) = g'(\infty,t^*) = G(\infty,t^*) = 1. \tag{11}$$

The initial conditions are given by the steady-state equations, obtained by putting $t^* = 0$ and $\partial/\partial t^* = 0$ in Eqs. (8)–(10). The steady-state equations are given by

$$2f''' + ff'' - \beta gg'' = 0, \tag{12}$$

$$2\lambda g''' + fg'' - f''g = 0, \tag{13}$$

$$2\mathrm{Pr}^{-1}G'' + fg' = 0. \tag{14}$$

The boundary conditions for Eqs. (12)–(14) are expressed as

$$f(0) = f'(0) = g(0) = g''(0) = G(0) = 0, \\ f'(\infty) = g'(\infty) = G(\infty) = 1. \tag{15}$$

Here η is the dimensionless independent variable; Ψ and f are the dimensional and dimensionless stream functions, respectively; t^* is the dimensionless time; ϕ and g are, respectively, the dimensional and dimensionless magnetic stream functions, respectively; F' and g' are the dimensionless velocity and induced magnetic field in x-direction, respectively; β is the magnetic force number which is the square of the ratio of the Alfven speed to the free stream velocity. λ is the reciprocal of the magnetic Prandtl number which is the ratio of the viscous to the magnetic diffusivity, ϵ is the ratio of the wall to free stream velocities, and a prime denotes derivatives with respect to η.

In our analysis, we have taken the fluid to be finitely conducting and the plate to be non-conducting. Therefore, there will be no surface current sheet or equivalently, the tangential component of the magnetic field is continuous accross the interface. This condition is mathematically expressed as $(H_1)_y = 0$ when $y = 0$ which in dimensionless form can be expressed as $g'' = 0$, when $\eta = 0$ [5].

Like Glauert [4], Gribben [5] and Na [6], we have taken the values of the magnetic parameter β in the range $0 \leqslant \beta < 1$. This is consistent with the existence of the steady-state solution of the "super Alfven" flow. By this we mean a flow in which the free stream velocity u_∞ is larger than the Alfven wave speed $(H_0(\mu_0/\rho)^{1/2})$ i.e., $\beta < 1$. For "sub-Alfven" flow ($\beta > 1$), any disturbance within the boundary layer can propagate upstream by means of the Alfven waves, thereby making the flow phenomena unstable [4].

It may be remarked that the steady-state equations (12) and (13) along with boundary conditions (15) are identical to those of Das [11]. Also, Eqs. (12)–(14) are essentially the same as those

of Glauert [4], Na [6] and Tan and Wang [7] who used slightly different transformations and the boundary conditions (i.e., they have used $g'(0)=0$ instead of $g''(0)=0$).

The skin friction and heat transfer coefficient are given by

$$\begin{aligned} C_{\mathrm{f}} &= 2\tau_{\mathrm{w}}/\rho u_{\infty}^2 = 2(\mathrm{Re}_x)^{-1/2} f''(0,t^*), \\ \mathrm{Nu} &= x(\partial T/\partial y)_{\mathrm{w}}/(T_{\infty}-T_{\mathrm{w}}) = (\mathrm{Re}_x)^{1/2} G'(0,t^*), \end{aligned} \tag{16a}$$

where

$$\tau_{\mathrm{w}} = \mu(\partial u/\partial y)_{\mathrm{w}}, \quad \mathrm{Re}_x = u_{\infty}x/\nu. \tag{16b}$$

Here C_{f} and Nu are the local skin friction coefficient and the local Nusselt number, respectively; Re_x is the local Reynolds number; τ_{w} the shear stress at the wall; and μ is the coefficient of dynamic viscosity.

3. Numerical method

We have solved the parabolic partial differential equations (8)–(10) under the boundary conditions (11) and initial conditions (12)–(15) by using an implicit, iterative, tridiagonal finite-difference method similar to that discussed by Blottner [14]. All the first order derivatives with respect to t^* are replaced by two-point backward difference formulae of the form

$$\partial A/\partial t^* = (A_{m,n} - A_{m-1,n})/\Delta t^*, \tag{17}$$

where A is any dependent variable and m and n are node locations along the t^* and η directions, respectively. The third-order differential equations (8) and (9) are converted into second order by substituting $V=f'$ and $H=g'$, respectively. Then, all the second-order equations for V, H and G are discretized using three-point central difference quotients while all the first-order differential equations are discretized by using the trapezoidal rule. At each line of constant t^*, a system of algebraic equations results. With the non-linear terms evaluated at the previous iteration, the algebraic equations are solved by using the well-known Thomas algorithm (see [14]). The same process is repeated for the next t^* value and the problem is solved line by line until the desired t^* value is reached. A convergence criterion based on the relative difference between the current and the previous iteration is employed. When this difference reaches 10^{-5}, the solution is assumed to have converged and the iteration process is terminated. A representative set of numerical results is shown graphically in Figs. 1–8 to illustrate the influence of various parameters on the solution.

4. Results and discussion

In order to assess the accuracy of our method we have compared the surface stress ($f''(0)$) and x-component of the induced magnetic field at the surface ($g'(0)$) when $t^*=0$ (steady-state case) with those of Glauert [4], Na [6] and Das [11]. For direct comparison with those of Glauert [4] and Na [6], we have to multiply $f''(0)$ by 4 and $g'(0)$ by 2. We have also compared our heat transfer

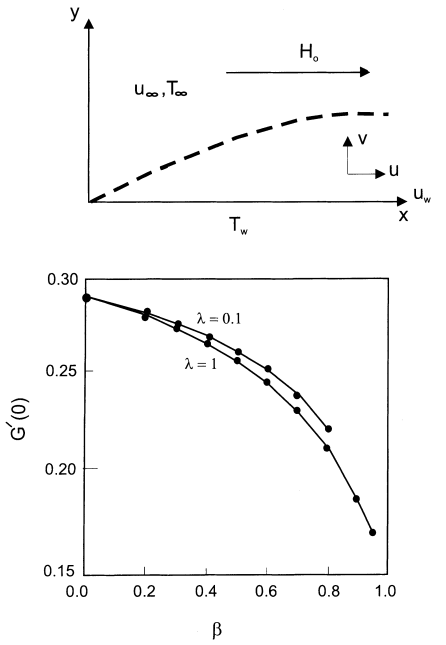

Fig. 1. Comparison of the heat transfer results ($G'(0)$) for the steady-state case ($t^* = 0$) with those of Tan and Wang for $\mathrm{Pr} = 0.7$;(_____) present results; (•), Tan and Wang.

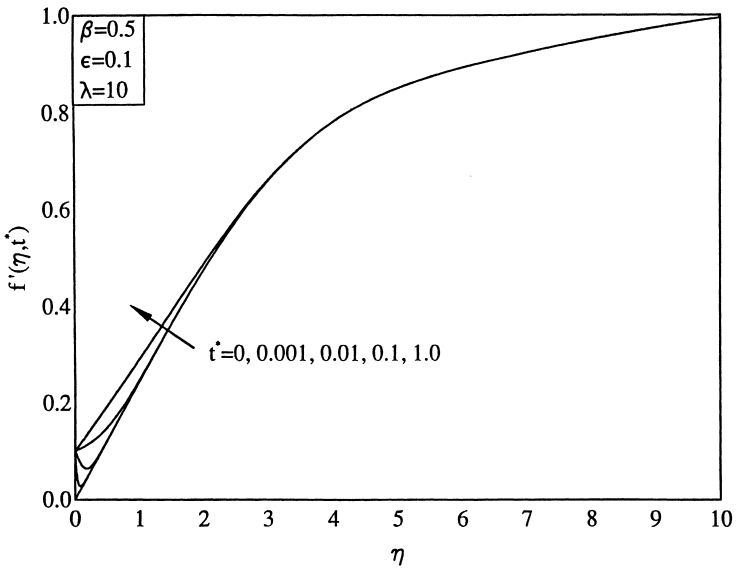

Fig. 2. Variation of the velocity profiles $f'(\eta, t^*)$ with time t^* for $\beta = 0.5$, $\lambda = 10$, $\varepsilon = 0.1$.

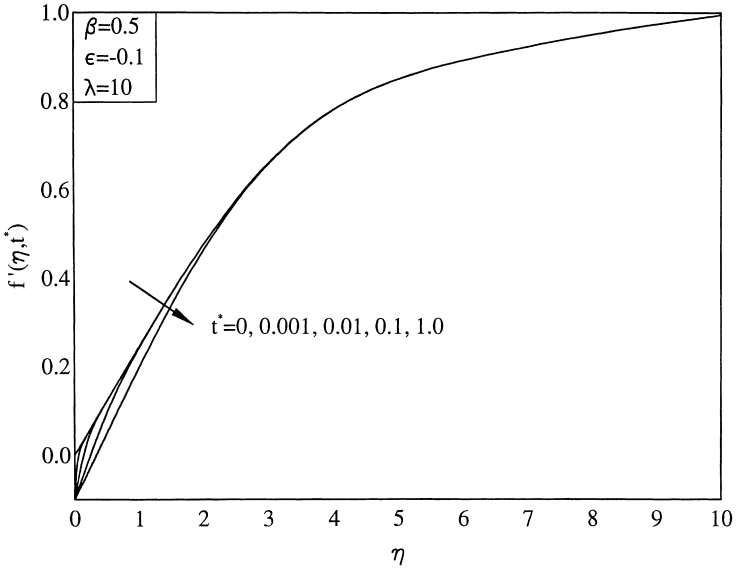

Fig. 3. Variation of the velocity profiles $f'(\eta, t^*)$ with time t^* for $\beta = 0.5$, $\lambda = 10$, $\varepsilon = -0.1$.

parameter on the surface ($G'(0)$) with that of Tan and Wang [7]. In all the cases, the results are found to be in very good agreement except with those of Das [11] where the maximum difference is found to be about 8%. This difference is attributed to the fact that Das [11] has used an approximate method for the solution of the governing equations. For comparison with the results of Das [14], we have used two different methods, namely, finite-difference method and fourth-order Runge–Kutta procedure. The comparison is shown in Tables 1 and 2 and Fig. 1.

Here the stress is on the temporal development of the boundary layer flow in a small interval of time $0 < t^* < t_1$ because significant changes take place only in a small interval of time after the start of the impulsive motion and the steady state is reached after certain time.

The variation of the velocity profiles $f'(\eta,t^*)$ with time t^* for $\beta = 0.5$, $\lambda = 10$ and $\varepsilon = 0.1$ (i.e., when the flat plate is impulsively moved in the same direction as the free stream velocity) is shown in Fig. 2 and for $\varepsilon = -0.1$ (i.e., when the plate is suddenly moved in the opposite direction to the free stream) in Fig. 3. It is observed that in a small interval of time t^* ($0 < t^* \leqslant 0.01$), the velocity near the wall is less than the velocity at the wall when $\varepsilon = 0.1$ (Fig. 2). This is known as the velocity defect. The physical reason for the velocity defect is that at $t^* = 0$, the plate is stationary ($f' = 0$ at $\eta = 0$) and the velocity f' increases monotonically from zero at $\eta = 0$, to 1 as $\eta \to \infty$. At $t^* > 0$, the plate is suddenly moved. Hence in a small interval of time the velocity of the fluid near the wall is less than that at the wall. There is no velocity defect when the plate is moved in the opposite direction to that of the free stream velocity (Fig. 3). For both cases ($\varepsilon = \pm 0.1$), the velocity $f'(\eta, t^*)$ changes with time t^* only in a small region near the wall ($0 \leqslant \eta \leqslant 2$), because the effect of the (small) wall velocity on the fluid is confined in a small region near the wall. Beyond this region the effect is small. Since the induced magnetic field in x-direction $g'(\eta,t^*)$ and temperature $G(\eta, t^*)$ change very little with t^*, they are not shown here. The reason for this behaviour is that the effect of the wall velocity on $g'(\eta, t^*)$ and $G(\eta, t^*)$ is indirect.

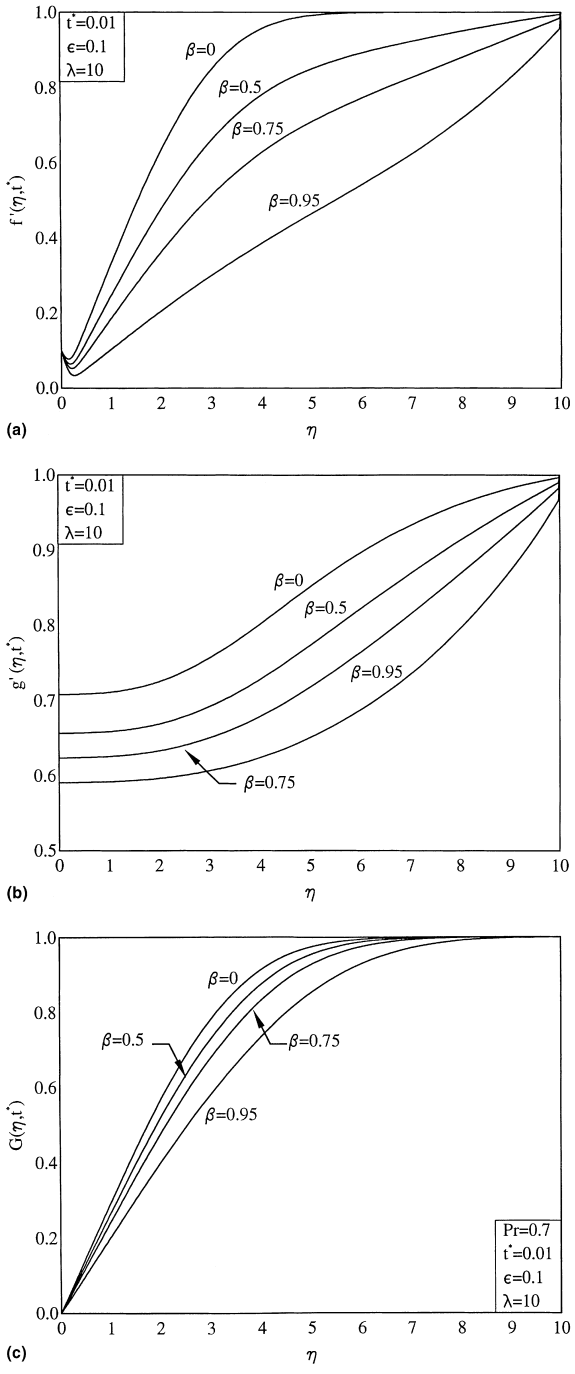

Fig. 4. Effect of the magnetic parameter β on the velocity profiles $f'(\eta, t^*)$, the x-component of the induced magnetic field $g'(\eta, t^*)$ and the temperature profiles $G(\eta, t^*)$ for $t^* = 0.01$, $\varepsilon = 0.1$, $\lambda = 10$, $\mathrm{Pr} = 0.7$. (a) $f'(\eta, t^*)$, (b) $g'(\eta, t^*)$ and (c) $G(\eta, t^*)$.

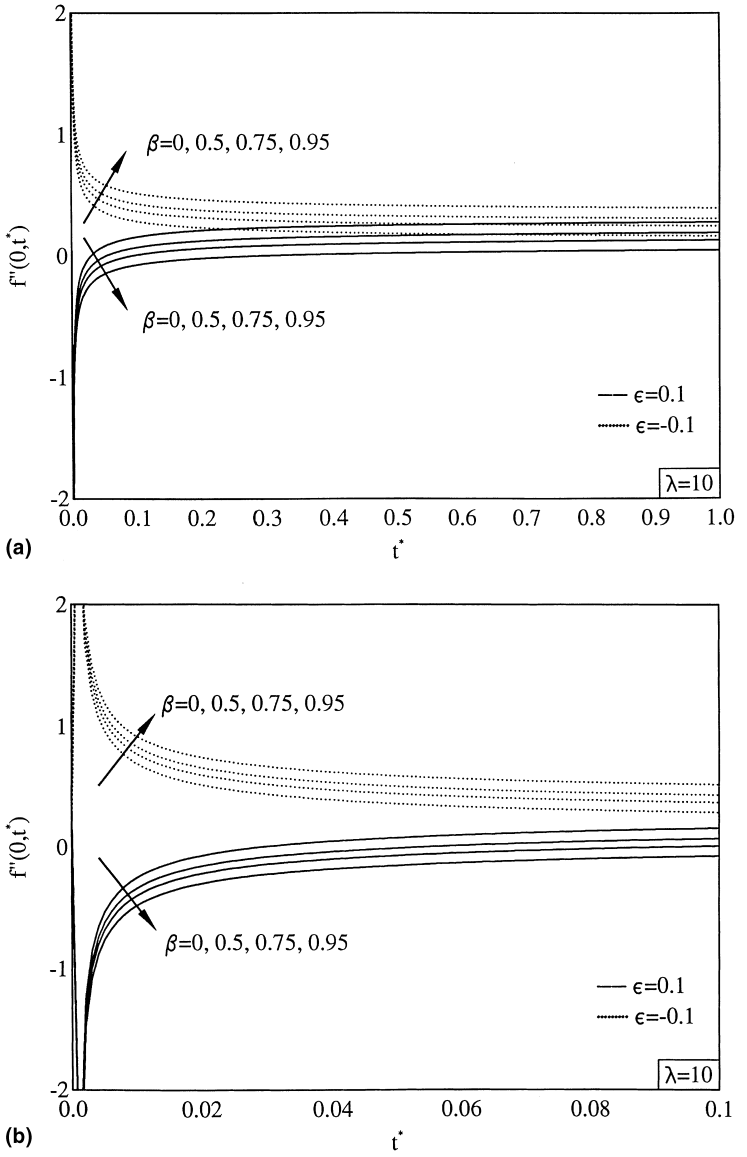

Fig. 5. Temporal development of the surface shear stress $f''(0, t^*)$ for $0 \leqslant \beta \leqslant 0.95$, $\varepsilon = \pm 0.1$, $\lambda = 10$; (a) $f''(0, t^*)$ for $0 \leqslant t^* \leqslant 1$; (b) $f'(0, t^*)$ for $0 \leqslant t^* \leqslant 0.1$.

The effect of the variation of the magnetic parameter β on the velocity profiles $f'(\eta, t^*)$, the x-component of the induced magnetic field profiles $g'(\eta, t^*)$ and the temperature profiles $G(\eta,t^*)$ for $t^* = 0.01$, $\varepsilon = 0.1$, $\lambda = 10$, $\mathrm{Pr} = 0.7$ is presented in Fig. 4(a)–(c). The effect of the magnetic parameter β on $f'(\eta,t^*)$, $g'(\eta,t^*)$ and $G(\eta, t^*)$ is found to be quite significant. Also, $f'(\eta, t^*)$, $g'(\eta, t^*)$ and $G(\eta, t^*)$ reduce with increasing β and the velocity, magnetic and thermal boundary layer thicknesses increase. This is due to the fact that increasing the magnetic parameter β results in a higher

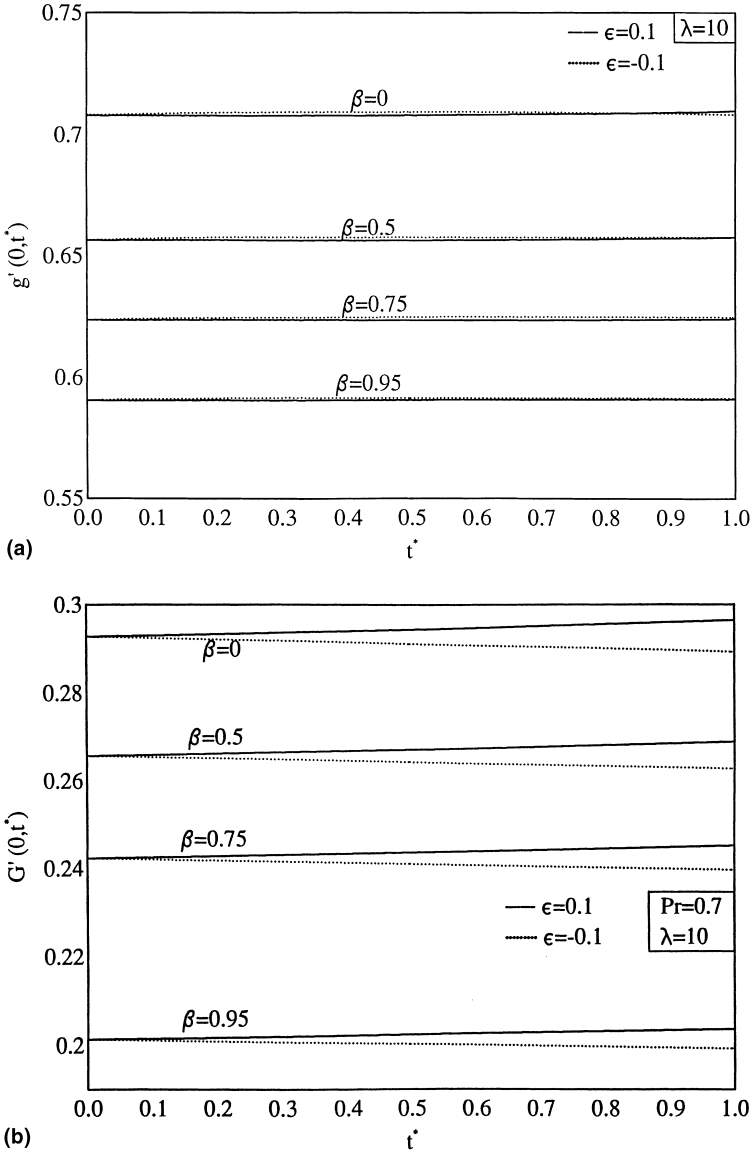

Fig. 6. Temporal development of the x-component of the induced magnetic field on the surface $g'(0, t^*)$ and the surface heat transfer $G'(0, t^*)$ and the effect of the magnetic parameter on $g'(0, t^*)$ and $G'(0, t^*)$ for $\varepsilon = \pm 0.1$, $\lambda = 10$, $\mathrm{Pr} = 0.7$, $\beta = 0$, 0.5, 0.75, 0.95 (a) $g'(0, t^*)$, (b) $G'(0, t^*)$.

Lorentz force which oppose the fluid motion. Similar trend was observed by Glauert [4] and Na [6] for the steady-state case without the temperature field. We also observe the velocity defect near the wall and this phenomenon has been explained earlier.

The variation of the surface shear stress ($f''(0,t^*)$) with time $t^*(0 \leqslant t^* \leqslant 1)$ for $0 \leqslant \beta \leqslant 0.95$, $\varepsilon = \pm 0.1$, $\lambda = 10$ is presented in Fig. 5(a). Since changes are more pronounced in a small time interval ($0 \leqslant t^* \leqslant 0.1$), the variation of $f''(0, t^*)$ with t^* in a small interval is shown in Fig. 5(b). For

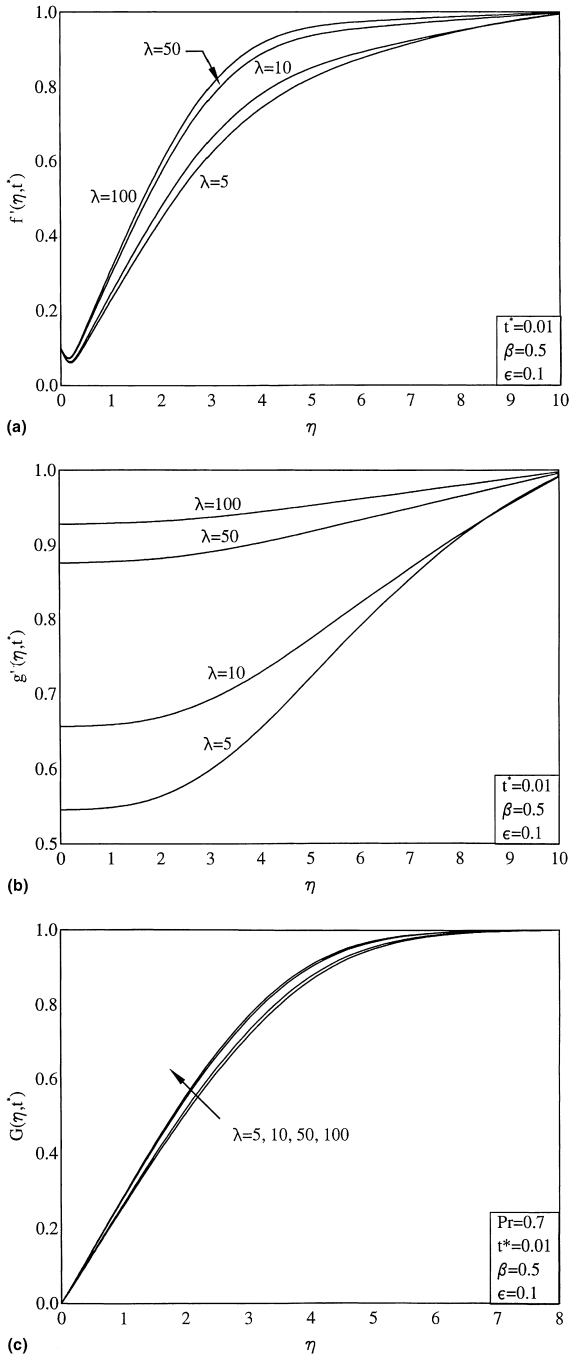

Fig. 7. Effect of the reciprocal of the magnetic Prandtl number λ on the velocity profiles $f'(\eta, t^*)$, the x-component of the induced magnetic field $g'(\eta, t^*)$ and the temperature profiles $G(\eta, t^*)$ for $t^* = 0.01$, $\beta = 0.5$, $\varepsilon = 0.1$, $\mathrm{Pr} = 0.7$. (a) $f'(\eta, t^*)$, (b) $g'(\eta, t^*)$ and (c) $G(\eta, t^*)$.

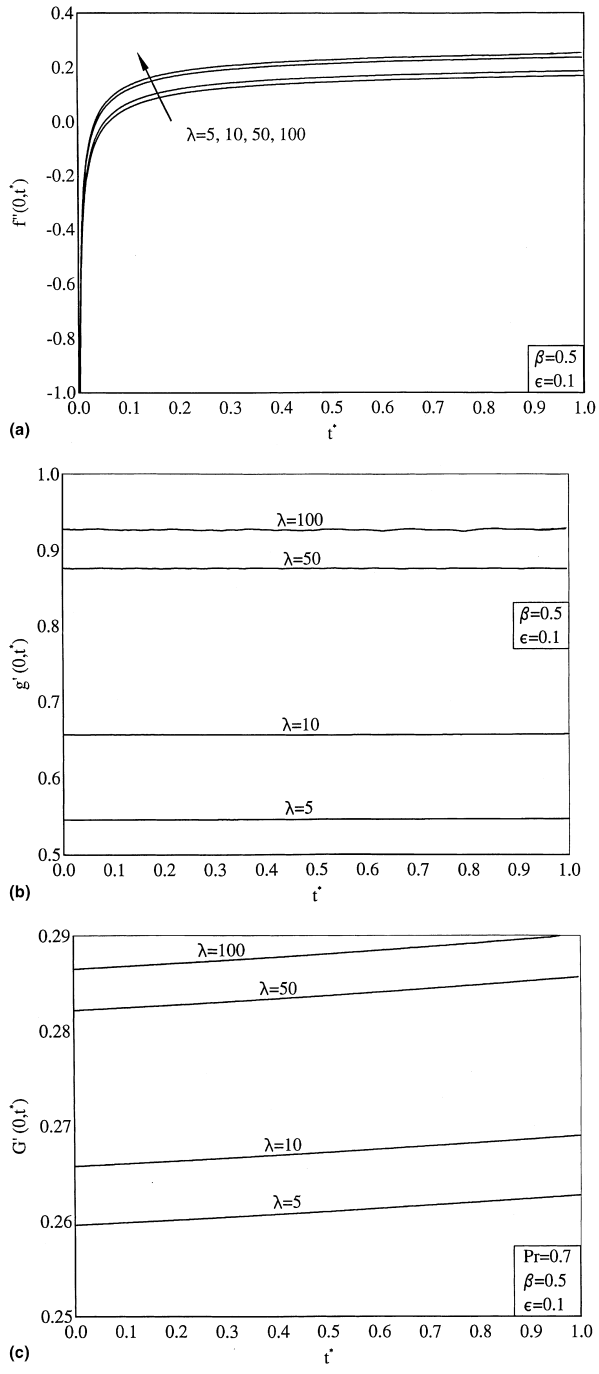

Fig. 8. Effect of the reciprocal of the magnetic Prandtl number λ on the surface shear stress $f''(0, t^*)$, the x-component of the induced magnetic field $g'(0, t^*)$ and the surface heat transfer $G'(0, t^*)$ for $\beta = 0.5$, $\varepsilon = 0.1$, $\mathrm{Pr} = 0.7$. (a) $f''(0, t^*)$, (b) $g'(0, t^*)$ and (c) $G'(0, t^*)$.

Table 1
Comparison of the surface shear stress $f''(0)$ and the x-component of the induced magnetic field at the surface $g'(0)$ for $t^* = 0$, $\lambda = 0.1$

β	$f''(0)$			$g'(0)$		
	Present results	Na [6]	Glauert [4]	Present results	Na [6]	Glauert [4]
0.0060	1.3239	1.3239	1.3238	0.4903	0.4903	0.4915
0.0181	1.3149	1.3149	1.3151	0.4882	0.4882	0.4892
0.0602	1.2829	1.2829	1.2839	0.4811	0.4810	0.4808
0.1792	1.1891	1.1892	1.1918	0.4593	0.4592	0.4557
0.2960	1.0910	1.0911	1.0946	0.4358	0.4356	0.4284
0.3535	1.0404	1.0402	1.0438	0.4231	0.4229	0.4139
0.4103	0.9883	0.9880	0.9915	0.4099	0.4097	0.3986
0.4659	0.9343	0.9341	0.9379	0.3963	0.3960	0.3828

Table 2
Comparison of the surface shear stress $f''(0)$ and the x-component of the induced magnetic field on the shear $g'(0)$ with those of Das [11] for $t^* = 0$ (steady-state case), $\beta = 0.3$

λ	$f''(0)$	$f''(0)$	$f''(0)$	$g'(0)$	$g'(0)$	$g'(0)$
	[11]	Finite-difference	Runge–Kutta	[11]	Finite-difference	Runge–Kuuta
0.4	0.24000	0.25833	0.26345	0.29010	0.31220	0.32012
2	0.30183	0.26313	0.26858	0.93849	0.32020	0.32326
4	0.30558	0.27315	0.27332	0.97076	0.55560	0.55851
10	0.30766	0.28472	0.28517	0.98862	0.67869	0.68824
15	0.30810	0.29170	0.29231	0.99246	0.73852	0.74020
25	0.30846	0.30067	0.30203	0.99549	0.80628	0.81564
100	0.30885	0.31955	0.32172	0.99888	0.92818	0.93900
400	0.30895	0.32687	0.32826	0.99971	0.97028	0.97830

$\varepsilon = 0.1$ and $0 < t^* < 0.04$, the surface shear stress $(f''(0,t^*)) < 0$ for all values of the magnetic parameter, because there is a velocity defect in the velocity profiles $f'(\eta, t^*)$ as mentioned earlier. However, for $\varepsilon = -0.1$, $f''(0, t^*)>0$. In both the cases ($\varepsilon = \pm 0.1$), the final steady state is reached quickly.

Fig. 6(a) and (b) show the temporal development of the x-component of the induced magnetic field on the surface ($g'(0, t^*)$) and the surface heat transfer ($G'(0, t^*)$) for $\varepsilon = \pm 0.1$, $\lambda = 10$, $\mathrm{Pr} = 0.7$. These figures also show the effect of the magnetic parameter β on $g'(0, t^*)$ and $G'(0, t^*)$. It is seen that $g'(0, t^*)$ and $G'(0, t^*)$ vary little with time t^* or ε, because the effect of the impulsive motion of the wall on the them is indirect. However, the magnetic parameter β strongly affects them and they reduce significantly with increasing β. The reason for such a behaviour is that the magnetic parameter β retards the fluid motion and thereby increases both the magnetic and thermal boundary layers.

Fig. 7(a)–(c) present the effect of the reciprocal of the magnetic Prandtl number λ on the velocity profiles ($f'(\eta, t^*)$), the x-component of the induced magnetic field profiles ($g'(\eta, t^*)$) and the temperature profiles ($G(\eta, t^*)$) for $\beta = 0.5$, $\varepsilon = 0.1$, $t^* = 0.01$, $\mathrm{Pr} = 0.7$. It is observed from these profiles that the effect of λ is more pronounced on $g'(\eta, t^*)$ and its effect on $G(\eta, t^*)$ is very small. This is because λ occurs in the equation for the induced magnetic field (see Eq. (9) and its effect on $G(\eta, t^*)$ is indirect.

The effect of the reciprocal of the magnetic Prandtl number λ on the surface shear stress ($f''(0, t^*)$), the x-component of the induced magnetic field on the surface ($g'(0, t^*)$) and the surface heat transfer ($G'(0, t^*)$) for $\beta = 0.5$, $\varepsilon = 0.1$, $\mathrm{Pr} = 0.7$ is illustrated in Fig. 8(a)–(c). The surface shear stress ($f''(0, t^*)$), the x-component of the induced magnetic field on the surface ($g'(0,t^*)$) and surface heat transfer ($G'(0, t^*)$) increase with λ, but the effect is more pronounced on $g'(0, t^*)$ because λ occurs in the equation governing the induced magnetic field (see Eq. (9)). As λ increases, the electrical conductivity (σ) decreases and the boundary layer velocity begins to lose control over the magnetic lines of forces. Consequently, the induced normal component of the magnetic field decreases and along with it the Lorentz force, which resists the fluid motion parallel to the plate, is reduced. This tends to increase the velocity and surface shear stress [4]. Further, the induced magnetic field on the surface ($g'(0, t^*)$) and the temperature $G(\eta, t^*)$ along with the surface heat transfer also increase with λ.

5. Conclusions

It is evident form the results that the effect of the impulsive motion of the flat plate is more pronounced on the surface shear stress than on the surface heat transfer and the x-component of the induced magnetic field on the surface. When the plate is impulsively moved in the same direction as that of the free stream velocity, velocity defect occurs in the velocity profiles whereas there is no velocity defect when the plate is moved in the opposite direction to the free stream velocity. The steady state is attained rather quickly after the start of the impulsive motion. The surface shear stress, the surface heat transfer and the x-component of the induced magnetic field on the surface decrease with an increasing magnetic field, but they increase with the reciprocal of the magnetic Prandtl number. However, the effect of the reciprocal of the magnetic Prandtl number is more pronounced on the x-component of the magnetic field.

References

[1] B.C. Sakiadis, A.I.Ch.E.J. 7 (1961) 221.
[2] H. Blasius, Z. Math u. Phys. 56 (1908) 1.
[3] H.P. Greenspan, G.F. Carrier, J. Fluid Mech. 6 (1959) 77.
[4] M.B. Glauert, J. Fluid Mech. 10 (1961) 276.
[5] R.J. Gribben, Proc. Roy. Soc. A 287 (1965) 123.
[6] T.Y. Na, Aeronaut. Quart. 21 (1970) 91.
[7] C.W. Tan, C.T. Wang, Int. J. Heat Mass Transfer 11 (1968) 319.
[8] N. Afzal, Int. J. Heat Mass Transfer 15 (1972) 863.
[9] K. Vajravelu, Acta Mechanica 64 (1986) 179.
[10] H.S. Takhar, M. Kumari, G. Nath, Mech. Res. Comm. 16 (1989) 257.
[11] U.N. Das, Proc. Camb. Phil. Soc. 68 (1970) 509.
[12] D.B. Ingham, J. Inst. Maths. Appl. 20 (1977) 459.
[13] M. Goyal, J.L. Bansal, Proc. Nat. Acad. Sci. India 62A (1993) 367.
[14] F.G. Blottner, AIAA.J. 8 (1970) 193.
[15] A.C. Eringen, G.A. Maugin, Electrodynamics of Continua II, Springer, Berlin, 1990.